10 July 2008

COMPASS Status Report 2008

The COMPASS Collaboration

Abstract

An overview of the 2007 COMPASS run with muon beam is given. The new physics results released during the last year are shortly described. The status of preparation of the 2008 run with hadron beam is discussed.

1 Overview of the COMPASS 2007 muon run

The COMPASS spectrometer was considerably upgraded in 2006 [1]. The only change for the 2007 running was the use of ammonia (polarised protons) as target material [2]. For the completion of the muon programme with a proton target, COMPASS had initially requested 9.5×10^{18} protons on the T6 target from SPS [3]. Assuming typical accelerator performances and an average intensity of 2×10^8 muons per spill, one 'proposal year' (i.e. 150 days) translates into $8.64 \times 10^{18} = P_{Ref}$ protons. Our request for completion was of $1.1 \times P_{ref}$ with a sharing of $0.3 \times P_{ref} = 2.6 \times 10^{18}$ for muon beam and Transversely (T) polarised target and $0.8 \times P_{ref} = 6.9 \times 10^{18}$ for muon beam and Longitudinaly (L) polarised target. Thanks to the particularly efficient beam delivery to fixed target experiments in 2007 a total of 7.2×10^{18} protons were provided to COMPASS, out of which 6.3×10^{18} could be used. The losses were mainly due to a leak in the ^{3}He circuit of the polarised target, which led to a partial blockage of the system, and required warming of the target. Discussions within the collaboration resulted in a change of the proposed sharing between T and L running in favour of the T running. Almost identical proton flux (3.1×10^8) was used for both T and the L data taking corresponding to 1.2 and 0.45 times the initially requested beam.

2 New physics results obtained with muon beam

2.1 $\Delta G/G$ from the 2002–2006 open charm data

The analysis of $\Delta G/G$ from charmed hadron production is now finalized for the full of 2002–2006 data set. The 2003 and part of the 2004 data have been reproduced implementing several improvements aiming at reducing the statistical error. The analysis uses a weighting by the analysing power a_{LL} and the signal-to-background ratio $\Sigma = S/(S+B)$. The quantity a_{LL} is obtained from a Neural Network (NN) trained on Monte Carlo events (Aroma). Due to enlarged acceptance in 2006, a new a_{LL} was built for the 2006 data analysis. Figure 1 shows the correlation between the a_{LL} reconstructed by NN and the one generated fom MC. The ratio Σ is parametrized in terms of the event kinematics. The weighting brings a significant improvement in statistical error due to the large variation of a_{LL} and Σ in phase space. In addition, some kinematic cuts can be less strict improving again the statistical error. A new cut has been introduced to reject electrons from the soft pion sample for D^* events using the RICH detector which reduces further the background. Figure 2 shows the weighted mass spectra for D^0 and D^* events for the four years of data taking. The total number of events is 37398 D^0 and 8675 D^*.
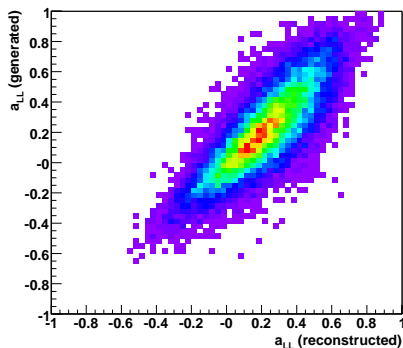

Figure 1: Correlation plot between the Monte Carlo a_{LL} and the reconstructed one.
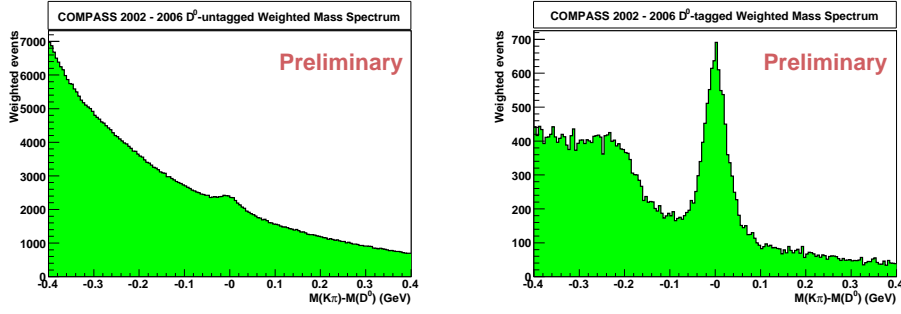
Figure 2: The weighted mass spectrum for D^0 *(left)* and D^* *(right)* for the 2002-2006 data.

Figure 3 shows the results of the Σ parametrisation and illustrates the large variation of the signal versus the background in the spectrometer acceptance.
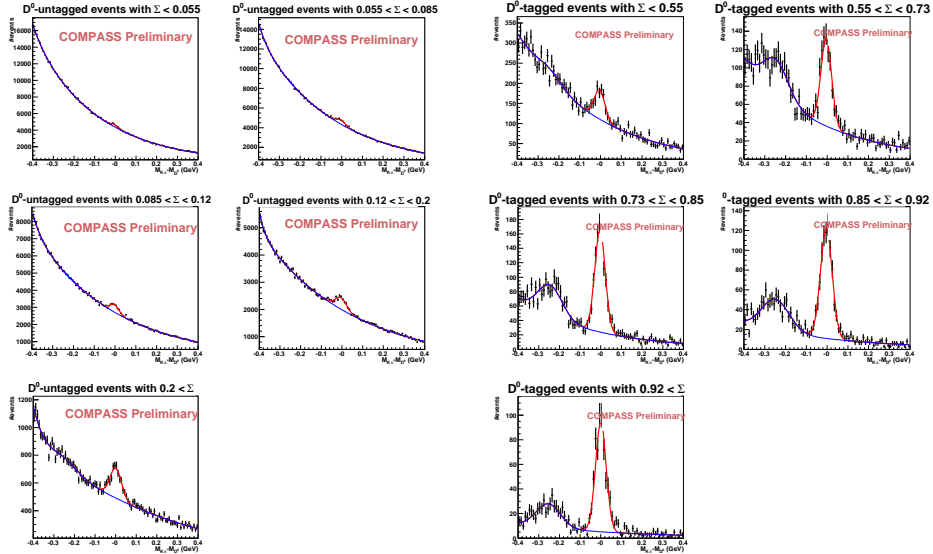

Figure 3: The weighted mass spectrum for D^0 *(left)* and D^* *(right)* for different bins in $\Sigma = S/(S + B)$.

The final value for $\Delta G/G$ using the D^0 and the D^* data is:

$$\Delta G/G = -0.49 \pm 0.27 \ (stat) \ \pm 0.11 \ (syst)$$

corresponding to mean values of $\langle x_g \rangle \sim 0.11$ for the gluon and of $\mu^2 \sim 13 \ (\mathrm{GeV/c})^2$ for the QCD scale. The 2002-2004 result is given in Ref. [4] and the paper on the full data set will be submitted within the next two weeks. The latter also contains asymmetries in bins of the transverse momentum and energy of the D meson. This enables other groups to use our data without further knowledge about the spectrometer.

2.2 $\Delta G/G$ from the 2002–2004 high–p_T data

Calculating $\Delta G/G$ from high transverse momentum (high–p_T) hadron pair events necessitates an evaluation of the different contributions to this process: Leading Order (LO, absorption by a quark), QCD Compton (QCDC, gluon radiation by a quark) and Photon Gluon Fusion (PGF), the process sensitive to the gluon polarisation. The analysis uses a parameterisation based on a Neural Network trained on Monte Carlo events. This allows us to assign to each event a probability to originate from each of these sub-processes. The method, illustrated in Fig. 4 makes the best use of the statistics.
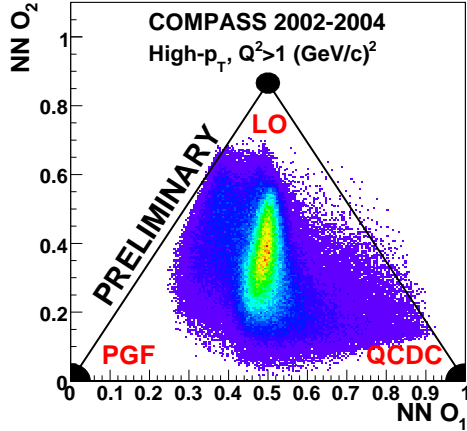

Figure 4: The two-dimensional output of the Neural Network for the estimation of the probability for a given event to originate from PGF, QCDC or PGF.

Figure 5 shows a comparison of the probabilities for the three sub-processes obtained with the NN parametrisation and from MC as a function of Σp_T^2. The agreement between the two evaluations is very good.
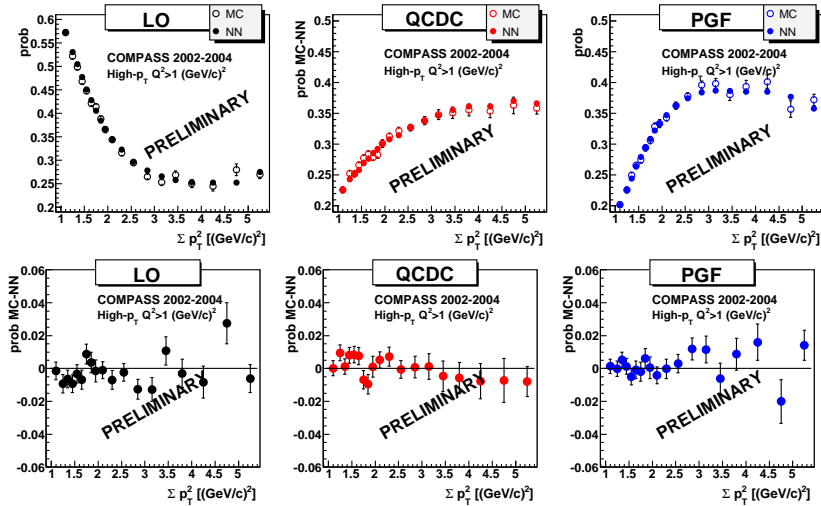

Figure 5: Neural Network and Monte Carlo comparison for R_{LO}, R_{QCDC} and R_{PGF} as a function of Σp_T^2.

Detailed studies of the systematics were performed including the dependence on the PDFs used in Monte Carlo, the inclusion of parton showers in order to (partly) simulate the effect of Next-to-Leading Order (NLO) processes. The final value for $\Delta G/G$ using the high p_T and $Q^2 > 1$ (GeV/c)^2 2002–2004 data sample is:

$$\Delta G/G = 0.08 \pm 0.10 \ (stat) \ \pm 0.05 \ (syst)$$

corresponding to mean values of $\langle x_g \rangle = 0.082$ for the gluon and of $\mu^2 \sim 3$ (GeV/c)^2 for the QCD scale.

Figure 6 shows the presently existing direct measurements of $\Delta G/G$, including the new results from COMPASS. The three blue lines show the GRSV parametrisation of $\Delta G/G$ as a function of x_g obtained from QCD fits to g_1 at $\mu^2 \sim 3$ (GeV/c)^2. The first Moments correspond, from top to bottom to: $\Delta G = 2.5$ (GRSV max), $\Delta G = 0.6$ (GRSV standard) and $\Delta G = 0.2$ (GRSV min). Our new results show a small value of the gluon polarisation in the region $0.04 < x_g < 0.2$ and are consistent with $|\Delta G| \sim 0.3 = 60\%$ of the nucleon [5].
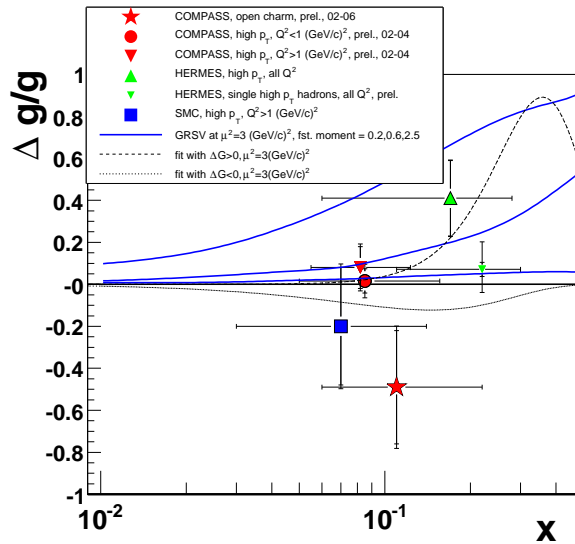

Figure 6: $\Delta G/G$ direct measurements from different experiments

2.3 Longitudinal polarisation of Λ and $\bar{\Lambda}$ from 2002-2004 data

The longitudinal spin transfer from the polarised beam muon (i.e. polarised virtual photon) to the Λ and $\bar{\Lambda}$ hyperons has been analysed for the 2003 and 2004 data. Figure 7 shows the invariant mass distributions and Fig. 8 shows the x_F distribution of the spin transfer to Λ and $\bar{\Lambda}$ for COMPASS data and other experiments.
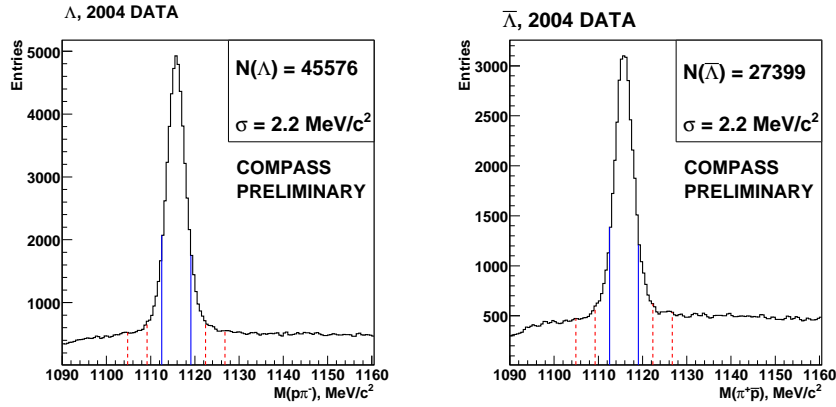

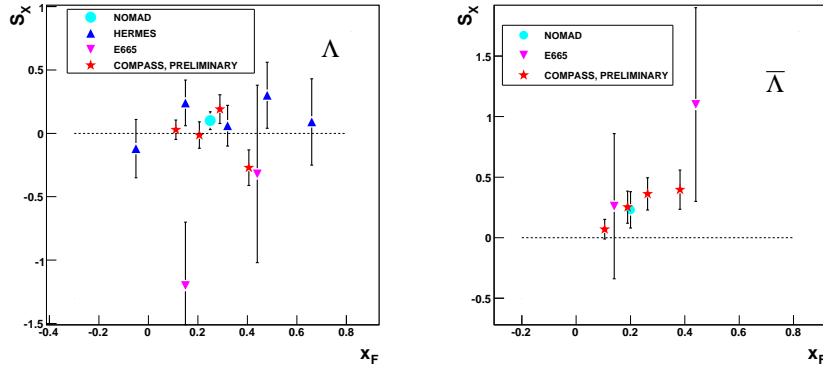Figure 7: The invariant mass distribution of Λ and $\bar{\Lambda}$ for the 2004 data.

Figure 8: The x_F distribution of the longitudinal spin transfer to Λ and $\bar{\Lambda}$ for the COMPASS 2003–2004 data (star) and other experiments, NOMAD (circle), E665 (reverse triangle) and HERMES (triangle).

Preliminary values for the spin transfer coefficients for the Λ, $\bar{\Lambda}$ and K_S^0 for the 2003-2004 data are:

$$S_X(\Lambda) = -0.012 \pm 0.047, \qquad S_X(\bar{\Lambda}) = 0.249 \pm 0.056, \qquad S_X(K_S^0) = 0.016 \pm 0.010.$$

COMPASS data confirms with better accuracy, the trend of a small spin transfer for the Λ and a strong positive one for the $\bar{\Lambda}$. Systematics is under study.

2.4 Azimuthal unpolarised (Cahn) asymmetries

Azimuthal asymmetries (for unpolarised target) have been measured for the 2004 COMPASS data sample. Modulations by $\cos(\Phi_h)$ and $\cos(2\Phi_h)$ arise due to the Cahn effect generated by a non-zero quark transverse momentum k_T and also from QCD contribution. The beam polarisation results in a $\sin(2\Phi_h)$ modulation. The three asymmetries have been measured,

using Monte Carlo to correct from acceptance effects. The $\cos(2\Phi)$ asymmetry can give access to the Boer-Mulders function which so far has not been measured. Figure 9 shows the comparison between the $\cos(\Phi)$ and $\cos(2\Phi)$ asymmetries and the predictions made for COMPASS kinematics.
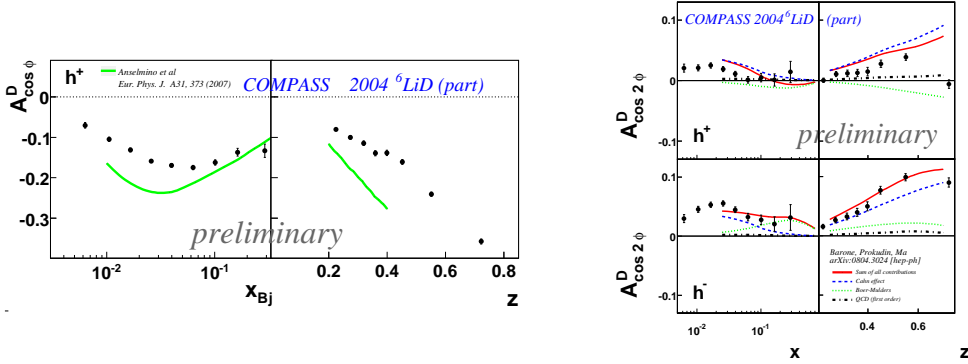

Figure 9: The $\cos(\Phi)$ asymmetry for positive hadron as a function of x_{Bj} and z compared to a theoretical prediction - green curve - *(left)*; the $\cos(2\Phi)$ asymmetry for positive hadrons (top) and negative hadrons (bottom) compared to a theoretical prediction - red curve - which includes the Cahn effect, the Boer–Mulders function and the QCD- first order term *(right)*.

2.5 Collins and Sivers asymmetries for K^0 production with transversely polarised deuteron (2002–2004 data)

In the scope of extracting the Collins and Sivers asymmetries for identified hadrons, asymmetries have been extracted for reconstructed K^0s. Figure 10 *(left)* shows the invariant mass of the hadron pair corresponding to a $V0$ vertex and the final cut on the invariant mass to identify a K^0. Figure 10 *(right)* shows the Collins and Sivers asymmetries, A_{Coll} and A_{Siv}, as a functions of x_{Bj}, z and p_T for the K^0 sample from the 2002-2004 data. The results for identified neutral and charged kaons and charged pions were submitted for publication [6].
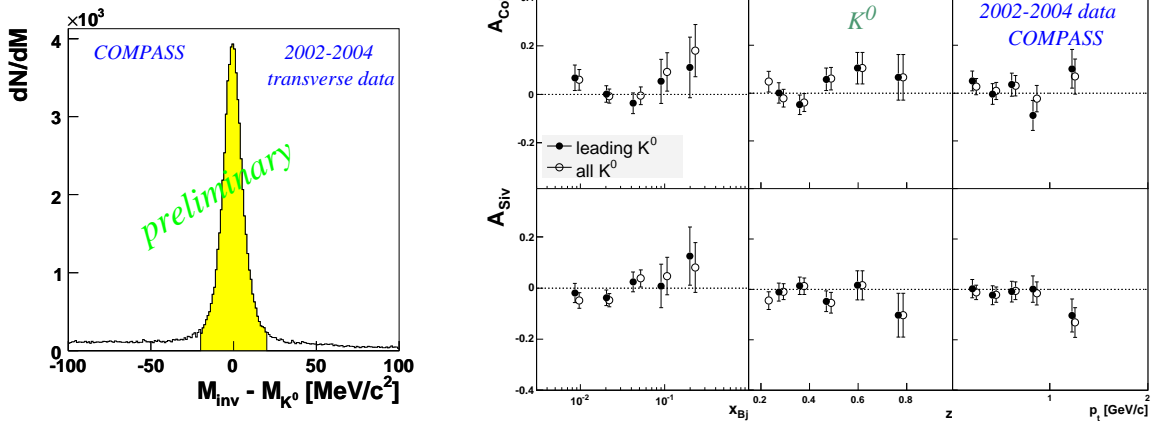

Figure 10: Invariant mass for the neutral kaon *(left)* and Collins and Sivers asymmetries for neutral kaons as a function of x_{Bj}, z and p_T *(right)*.

2.6 Collins and Sivers asymmetries for the proton from the 2007 data

The full statistics obtained in 2007 with the transversely polarised proton (NH3) target has been processed and a fraction of the data has been analysed. Due to some spectrometer instabilities a part of the data needs further studies. Great care has been devoted to scrutinize possible systematic effects and each step in analysis was cross-checked by three independent analyses. Figure 11 shows A_{Coll} as a function of x_{Bj}, z and p_T for positive and negative hadrons. The deviation from zero observed in the last high x_{Bj} bins was previously observed by HERMES. Due to the lower average Q^2 a debate arose, whether the effect is indeed due to transversity or rather a higher twist effect. The COMPASS result now confirms the existence of a non-zero transversity in the proton.
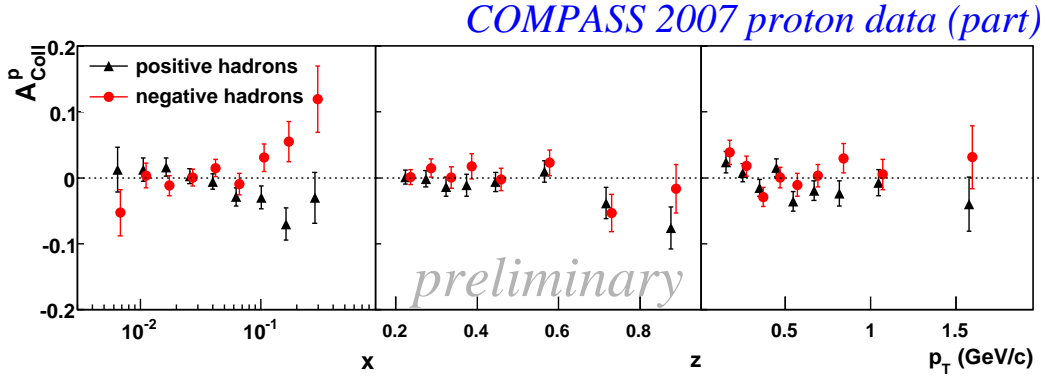

Figure 11: The Collins asymmetries A_{Coll} from the 2007 proton data as a function of x_{Bj}, z and p_T for positive and negative hadrons.

The observed Sivers asymmetries (Figure 12) are compatible with zero and smaller than those seen by HERMES, but still compatible with their result. A definitive conclusion can only be drawn after the analysis of our full set of data set which will yield about a twice higher precision.
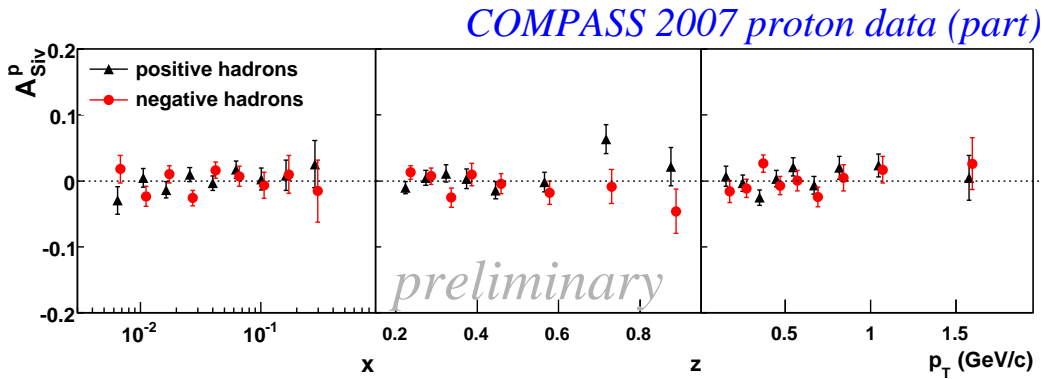

Figure 12: The Sivers asymmetries A_{Siv} from the 2007 proton data as a function of x_{Bj}, z and p_T for positive and negative hadrons.

The proton and deuteron data will be used together to perform a flavour separation of the transversely polarised quark distributions.

3 The preparation of the 2008 hadron run

A careful beam tuning by L. Gatignon resulted, as expected, in an about five times higher ratio of pions over primary protons, so that now there is no limitaion from the beam side. An important progress for the calibration of the electromagnetic calorimeters is the successful setting up to a low energy (10 GeV) electron beam covering the kinematical range of ECAL1. Substantial modifications of the spectrometer were implemented for the hadron run (see [7] sec.4). The two **Cedars detectors** installed at the end of the M2 beam line allow to select the pion or the kaon component ($\simeq 5\%$) of the beam. They are both operational and integrated into our read-out and trigger system. The final adjustment which requires a π beam with good parallelism has started. Optimal setting of slits and threshold has still to be established. Figure 13 shows in a logarithmic scale the results from a pressure scan, where the π and K components are clearly identified.
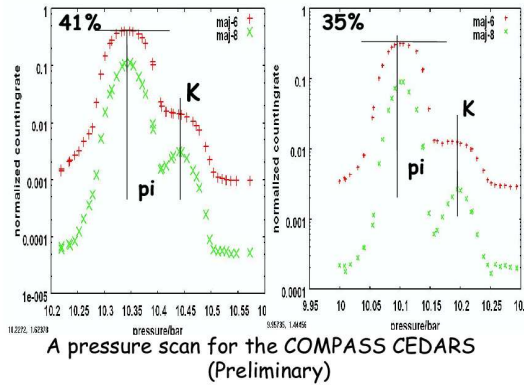

Figure 13: First results from the pressure scan of the two M2 beamline Cedar counters for 2 combinations of the Cherenkov counters.

The **Recoil proton Detector (RPD)** consists of an inner scintillator ring (A) and an outer ring (B). It surrounds the 40 cm long Liquid Hydrogen (LH) target inserted from the upstream side of the RPD as shown in Fig. 14 (*left*). The conical cryostat houses the downstream silicon telescope and is inserted from the downstream side into the RPD as shown in Fig. 14 (*right*). Three stations of silicon are placed upstream of the RPD. The LH target has been successfully installed and filled.
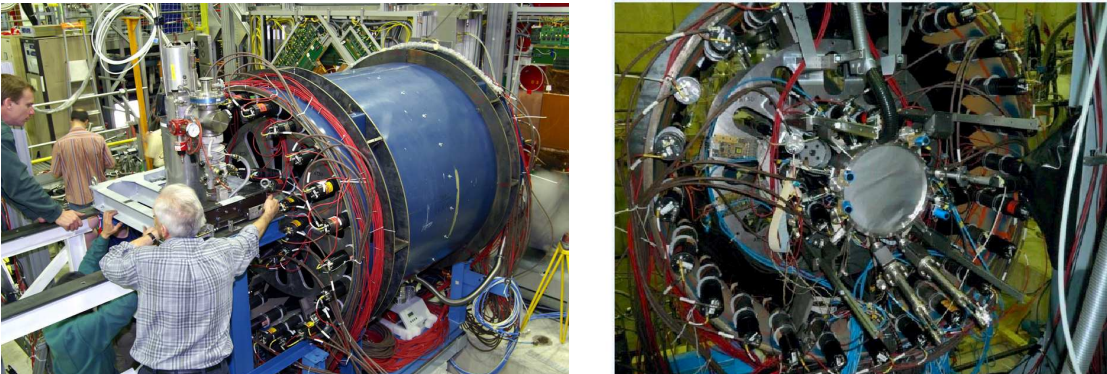

Figure 14: The Recoil Proton Detector: upstream side, the liquid hydrogen target *(left)*; downstream side, the conical cryostat for the cold silicon tracker *(right)*.

The RPD performs precise time-of-flight (ToF) measurements with an accuracy of ~ 350 ps and also amplitude measurements to identify protons, pions and electrons. It enters into the definition of the hadron trigger. The trigger electronics based on a FPGA system has been installed and is presently being adjusted. Calibration of the RPD is ongoing. Figure 15 shows a typical distribution of energy loss in the B scintillators versus the velocity β of the recoiling particle derived from the ToF between A_i and the corresponding B_{2i-1}, B_{2i} and B_{2i+1} counters.
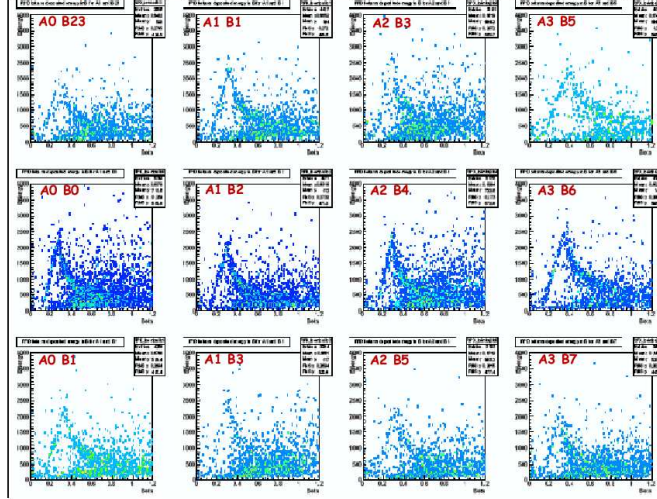

Figure 15: Energy loss in B counters versus velocity β for recoiling protons emitted from the liquid hydrogen target. The observed rise results from protons crossing the A counter and stopping in B while the drop is from proton exiting B and depositing decreasing amounts of energy.

The **silicon detectors** are cooled with liquid nitrogen in order to improve radiation hardness. The optimum temperature may be higher than the projected 130 K and tests are on-going on both the upstream and downstream silicon stations. Due to a mechanical problem, it was decided to operate the downstream silicon stations initially in a warm mode. Figure 16 shows the two-dimensional hit distribution in one of the new downstream silicon trackers and the corresponding hit profiles.
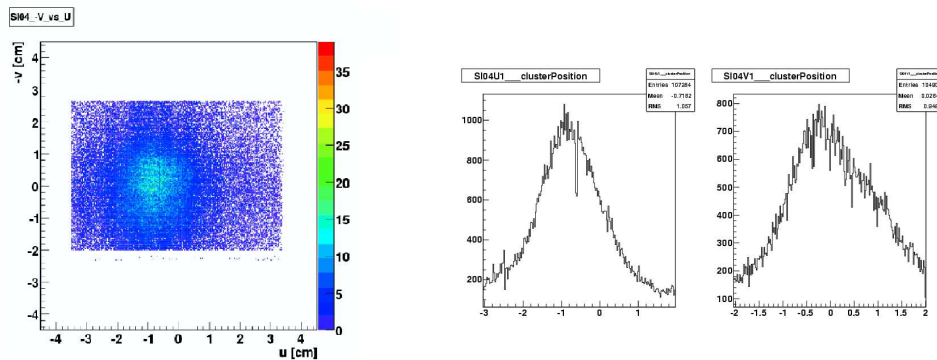

Figure 16: Hit distributions measured with a nominal intensity π beam hitting the liquid hydrogen target (detector installed in the downstream conical cryostat).

To minimise the amount of material along the beam path in order to reduce the background from secondary interactions, new detectors with a pixelized readout in the central region called **Pixel GEM** (PGEM) have been developed to replace a major fraction of the scintillating fibre detectors. One of the PGEM detector is shown in Fig. 17. The five PGEM (i.e. 3 stations) foreseen for the 2008 hadron run are now operational.

Pixel GEM detectors
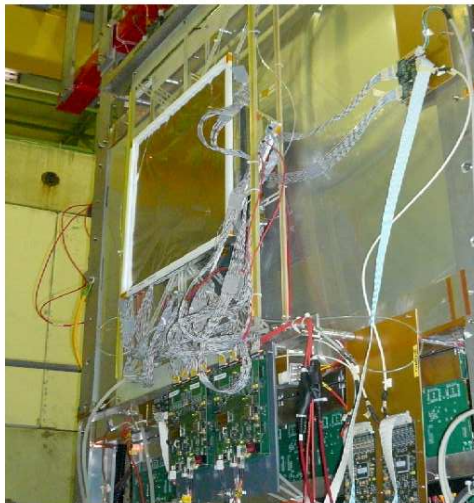
Upstream of SM1
PGEM01

Upstream of SM2
PGEM02
PGEM03

Downstream of SM2
PGEM04
PGEM05

Figure 17: One of the newly installed Pixel GEM *(left)* and the position of the 5 detectors in the spectrometer *(right)*.

The **hadron trigger** is an almost entirely new system which involves specific components. It provides the following functions:
- to define beam particles which enter the spectrometer and interact (**Cedars, beam counters, beam killer**),
- to select elastic proton vertex in the target (**beam counters, RPD, beam killer**),
- to exclude potentially incomplete events (**sandwich veto**),
- to reduce elastic events (**elastic veto, multiplicity trigger**),
- to require charge multiplicity ≥ 1 in the forward part of the spectrometer.

All trigger components are available and installed, however it still requires dedicated running time for commissioning and tuning.

Considerable work was done to improve the performances of the electromagnetic calorimeters **ECALs** (ECAL1 and ECAL2). In order to stand the high integrated radiation dose expected for the central part of ECAL2 with hadron beam, about 800 lead glass blocks were replaced by new radiation hard lead/scintillator modules (Shashlik modules) as shown in Fig. 18. The radiation hard lead glass blocks previously located in the ECAL2 center were moved to the outer part. De facto, the whole ECAL2 was completely reshuffled.
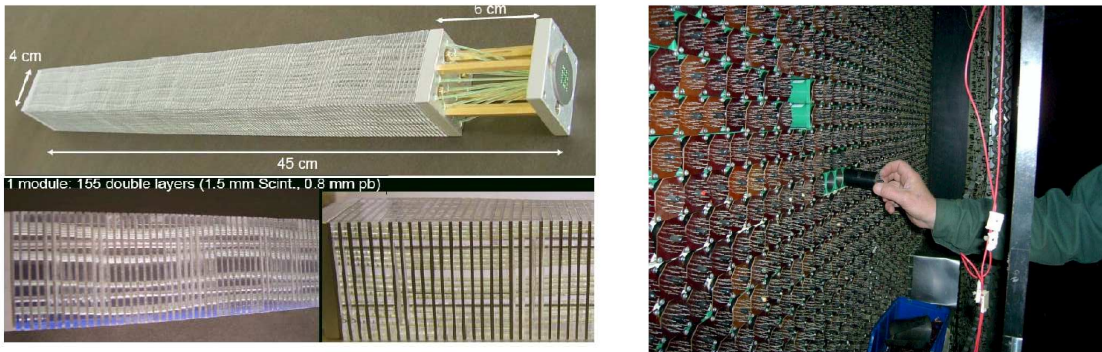
Figure 18: The new radiation hard lead/scintillator sampling calorimeter Shashlik modules *(left)*; a view from the downstream part of ECAL2 *(right)*.

Some modifications were also made in the spectrometer to reduce the amount of material in the acceptance of the ECALs in order to minimize the degradation of electromagnetic response.
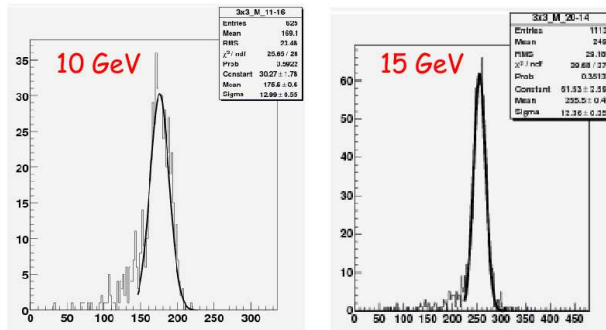

Figure 19: Calibration of ECAL1 using available electron beam of energy down to 10 GeV.

Figure 19 shows the response of ECAL1 to electrons of 10 GeV and 15 GeV. The calibration of ECAL1 with electrons has been fully completed and calibration of ECAL2 is near completion. Note that the read-out of ECAL2 has been upgraded, replacing the remaining "old" FIADCs converters by the more precise 12 bits SADCs converters which provide more accurate amplitude and also time measurements.

Beam was available for the commissioning of new hardware, calibrations and spectrometer studies starting May 30, corresponding to ~ 34 days of scheduled beam used until now (July 10) [8]. The final calibration of ECAL2 should be completed within the next days.

The beam time request for the 2008 hadron run submitted by COMPASS to SPSC [9] last year is reproduced in the table below. It shows that we are well within our planned schedule.

Beam time request for the 2008 run with hadron beam	
Commissioning of new hardware and trigger with beam	~ 30 days
Calorimeter calibration	~ 15 days
Diffractive production (neg. π beam)	~ 35 days
"Central" Production (pos. π/p beam)	~ 60 days

Finally, we recall the commitments agreed upon following the discussions with our Referees:
- in early spring 2009 we will provide a preliminary analysis of the $3 - \pi$ decay channel in the spin-exotic $\pi_1(1600)$ resonance region.
- for fast feed back from the central production measurements, we will concentrate on the 4-charged-π channel in the $f_0(1500)$ resonance region.
From the samples analyzed, the Monte Carlo studies and the known detector performances, we will present in early 2009 how well the physics goals of the 2008 run can be achieved.

References

[1] CERN-SPSC 2006-013, SPSC-SR-007, 18 April, 2006.

[2] CERN-SPSC 2007-024, SPSC-SR-022, 20 June, 2007.

[3] CERN-SPSC 2007-002, SPSC-M-754, 23 January, 2007.

[4] CERN-PH-EP/2008-003, hep-ex0802.3023.

[5] PLB 647 (2007) 8-17, The Deuteron Spin-dependent Structure Function g1d and its First Moment.

[6] CERN-PH-EP/2008-002, hep-ex0802.2160.

[7] CERN-SPSC 2007-015, SPSC-M-755, 12 April, 2007.

[8] http://ab-div.web.cern.ch/ab-div/Schedules/schedule2008.pdf

[9] CERN-SPSC 2007-037, SPSC-M-761, 29 November, 2007.